Available online at www.sciencedirect.com
ScienceDirect
Journal of Power Sources 164 (2007) 606–613
JOURNAL OF POWER SOURCES
www.elsevier.com/locate/jpowsour

Fuel sensor-less control of a liquid feed fuel cell system under steady load for portable applications

C.L. Chang [a,b,*], C.Y. Chen [a], C.C. Sung [b], D.H. Liou [a]

[a] *Institute of Nuclear Energy Research (INER), No. 1000, Wunhua Rd., Jiaan Village, Longtan Township, Taoyuan County 32546, Taiwan, ROC*
[b] *National Taiwan University, Taiwan, ROC*

Received 22 September 2006; received in revised form 30 October 2006; accepted 31 October 2006
Available online 4 December 2006

Abstract

This study presents a novel fuel sensor-less control scheme for a liquid feed fuel cell system that does not rely on a fuel concentration sensor. The proposed approach simplifies the design and reduces the cost and complexity of a liquid feed fuel cell system, and is especially suited to portable power sources, of which the volume and weight are important. During the reaction of a fuel cell, the cell's operating characteristics, such as potential, current and power are measured to control the supply of fuel and regulate its concentration to optimize performance. Experiments were conducted to verify that the fuel sensor-less control algorithm is effective in the liquid feed fuel cell system.
© 2006 Elsevier B.V. All rights reserved.

Keywords: Liquid feed fuel cell; Fuel sensor-less control; Direct methanol fuel cell

1. Introduction

A liquid feed fuel cell like direct methanol fuel cell (DMFC) has been a promising candidate for portable applications in recent years. DMFC differs from other power generating devices, such as PEMFC, in that the former uses methanol as fuel rather than hydrogen, since it has a higher energy density. Using liquid methanol as a fuel in the reaction eliminates the problem of hydrogen storage, and therefore, the risk of explosion of the fuel cells, significantly increasing both the convenience and safety of the fuel cells, and making DMFC more adaptable to portable power applications such as laptops, PDAs, camcorders and others.

The methanol concentration significantly influences the performance of the DMFC system. The power output becomes low and unstable when the methanol concentration falls below a predetermined range. When the methanol concentration surpasses that predetermined range, the output power may be sustained, but if the methanol concentration is excessive, then methanol crossover becomes an issue. DMFC suffers from methanol crossover from anode to cathode through the membrane of electrolyte, which causes considerable loss in fuel efficiency. Regulating the supply of fuel is essential in maintaining the methanol concentration in a predetermined range in which the DMFC system can operate optimally.

A fuel sensor, such as a methanol concentration sensor, is typically adopted to detect the concentration of methanol, providing information that can be used by the control system to judge appropriate timing for supplying methanol. Two types of methanol concentration sensor with different operating principles exist. The first type is based on electrochemical sensing; the second is based on physical sensing [1]. Important issues are associated with both. With respect to the electrochemical sensor, the issues are degradation of the MEAs and the deterioration of catalysts and electrodes over time. Accordingly, frequent calibrations are required to ensure accuracy and resolution [2]. The fuel sensor-based measurement system also raises stability and durability issues: a larger measurement uncertainty reduces the control accuracy. A physical sensor typically must be employed with auxiliary driving devices and other sensors, like a thermometer, in a measurement system. Meanwhile, physical sensors are generally temperature-dependent and require temperature compensation, increasing complexity of the measurement system and making the use of such a sensor more

* Corresponding author at: Institute of Nuclear Energy Research (INER), No. 1000, Wunhua Rd., Jiaan Village, Longtan Township, Taoyuan County 32546, Taiwan, ROC. Tel.: +886 3 4711400; fax: +886 3 4711409.
E-mail address: clchang@iner.gov.tw (C.L. Chang).

0378-7753/$ – see front matter © 2006 Elsevier B.V. All rights reserved.
doi:10.1016/j.jpowsour.2006.10.092

difficult. For example, the ultrasonic sensors have problems with changes in output sensitivity over temperature that result in poor differentiability [1]. Additionally, such experimental tasks as calibration are necessary when a physical sensor is adopted. Although this approach can be used to control the concentration of the fuel, it nevertheless has the shortcomings of increasing the complexity and the cost of a liquid feed fuel cell system.

Very little published literature exits on fuel sensor-less control over the liquid feed fuel cell that can aid in reducing the cost and complexity associated with the use of fuel concentration sensor. Acker et al. [3] provided a method for regulating the concentration of methanol based on the system's operating characteristics. One or more operating characteristics of the fuel cell, such as the open circuit potential, the potential at the anode near the end of the fuel flow path and the short circuit current of the fuel cell are used actively to control the concentration of methanol. The shortcoming of such an approach is that when the open circuit potential or the short circuit current is measured, the load must be opened or short-circuited, both of which actions require switching the power supply to the back up battery. Measurements must be made routinely to regulate fuel concentration while the battery supplies the power. Moreover, since a short circuit is periodically required to detect the current, the fuel cell can be easily damaged, affecting the stability of the fuel cell system. However, the aforementioned methods are based on predetermined measurements of the fuel cell system. The monitoring and control of the methanol concentration are loose, because of the complexity of the operation of fuel cells and the degradation of MEAs.

Zhang et al. [4] presented an indirect approach for determining the concentration of methanol in a fuel stream based on measurements of the temperature of the fuel stream as it enters the fuel cell stack, the operating temperature of the fuel cell stack and the load current. This approach is based on the predetermined measurement of the fuel cell system; it requires much effort to calculate the concentration of an operating DMFC system. The amount of calibration data should be large and these data must be stored in memory, increasing the volume and weight of the portable power sources. This scheme suffers from degradation of the MEA, and consequent performance degradation over time. Chiu and Lien [5] proposed an interpolation algorithm based on constant concentration surfaces to estimate the concentration of methanol in a DMFC system. This indirect measurement scheme can be utilized to determine the concentration of methanol but it also suffers from the degradation of the MEAs.

Given the disadvantage of the methods described above, the need to develop a better method for supplying fuel to a liquid feed fuel cell has become urgent. This work presents an impulse response based on discrete time fuel injection (IR-DTFI) control scheme, which provides easier and faster control based on an experimentally verified algorithm. The operating characteristics of the DMFC stack are applied to control the power generating system without the need to determine the concentration of fuel, and the approach can survive from the degradation of MEAs. The fuel can be a hydrogen-rich liquid fuel such as methanol, ethanol or another. DMFC is considered as an example for a liquid feed fuel cell, to demonstrate the IR-DTFI control algorithm.

2. System design and test rig

2.1. Fabrication of the bipolar plate

The bipolar plates and the membrane electrode assemblies (MEAs) are two main parts of a fuel cell stack. Graphite plates with thickness of 1.7 mm were used as bipolar plates. The bipolar plates serve to distribute air and methanol solution uniformly to the gas diffusion layers (GDLs) and MEAs, conducting current between the cells for current collection. The flow channels were milled in the graphite plates and the flow pattern was triple serpentine. The effective area of the MEA was approximately 25 cm^2. The bipolar plates were developed with regard to thickness, channel geometry configurations, contact resistance, and electricity conductivity yielding optimized configuration in volume and weight. The cells are connected electrically in series. The reactants are fed in parallel to the cells from two symmetrical manifolds. More details can be found in our previous work [6–8].

2.2. Fabrication of the stack and the membrane electrode assembly

The MEAs are made up from commercially available membranes (Nafion 117, DuPont). The anode and cathode electrode were coated with Pt-Ru/C ($\sim$2 mg cm^{-2}) and Pt/C ($\sim$2 mg cm^{-2}) catalysts, respectively. Two DMFC stacks with different number of cells (16-cell and 25-cell) were manufactured for experiments to verify IR-DTFI scheme. Under optimal conditions with respect to flow rate of reactants, temperature, and flow channel configurations, the average electricity output of the 16-cell stack is above 17 W.

2.3. The IR-DTFI control strategy for DMFC system

Fig. 1 described in the following shows the flow chart of the IR-DTFI strategy. Step A1 starts to determine a specific monitoring period according to the load. Fig. 2 plots the polarization curve of the fuel cell and explains how to determine the monitoring period. The power curve has a maximum power P_{max}, and the corresponding I_{max} is a suggested value for deciding the minimum duration for the specific monitoring period. The system control unit determines the specific monitoring period, at any constant current discharging condition, inversely proportional to I_{max}. In addition, the minimum specific monitoring period at I_{max} is predetermined through experiment. Therefore, the specific monitoring period is the duration that the fuel cell can sustain the load I_{max} within the injection of a specific amount of fuel. Step A2 feeds a specific amount of fuel into the mixing tank. Fig. 3 plots the measurement system, system control, and fuel-feeding unit for the verification and evaluation of the IR-DTFI control scheme.

Then, step A3 measures the operating characteristics of the fuel cell over the specific monitoring period. The operating characteristic value here can be potential, current, or power measured at the stack terminal. Step A4 obtains a first characteristic value during a time interval before the end of the specific monitoring

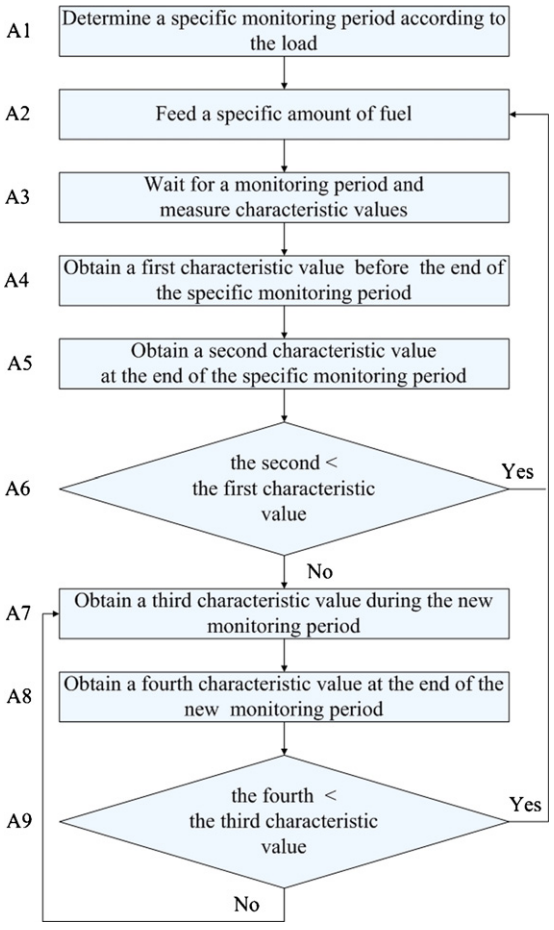

Fig. 1. Flow chart of the IR-DTFI control algorithm.

period. Then the flow proceeds to step A5 to obtain a second characteristic value at a time point that locates at the last of the specific monitor time interval. As seen from trend of operating characteristic of Fig. 7(b), the system control unit should have the capability to identify and determine whether the trend of operating characteristics are going upward or downward at the end of the specific monitoring period (T_0, T_1, T_2) from the relation between the first and the second characteristic value. From this point of view, a lot of way can define the first characteristic value. Therefore, step A6 compares the first with the second characteristic value to judge the trend. If the second is smaller than the first characteristic value that means the trend goes downward, the algorithm returns to step A2 to feed fuel

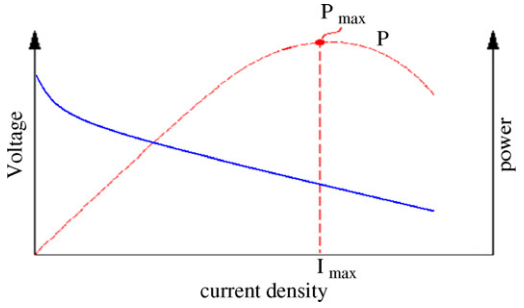

Fig. 2. Definition of P_{max} and I_{max} by polarization curve.

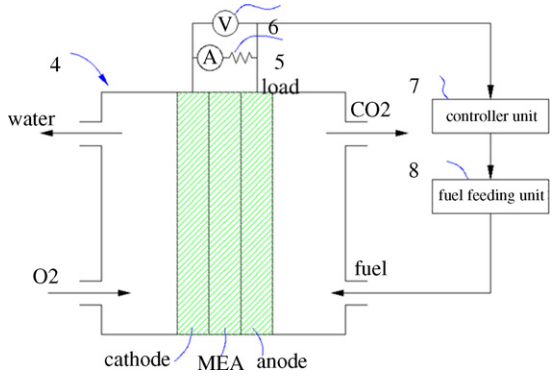

Fig. 3. Schematic diagrams of the measurement system, system control, and fuel-feeding unit for the verification and evaluation of the IR-DTFI control scheme.

to the mixing tank. It represents that the methanol concentration is insufficient for the mass transport of fuel at the end of the specific monitoring period as shown at point T_0, T_1 in Fig. 7(b).

When the trend is going upward, it means that there is excess fuel accumulated at the end of the specific monitoring period. The system control unit stops injecting fuel until the trend of operating characteristics goes downward. As shown in Fig. 7(b), the excess fuel is consumed during the injection delay period between T_2 and T_3. By way of the comparison method, the third and the fourth operating characteristics are set up to determine when the trend will going downward after the specific monitoring period mentioned above. If the second exceeds the first that means trend up, then the flow proceeds to step A7 to calculate a third characteristic value during the new period after the specific monitoring period. Then, step A8 obtains a fourth characteristic value at the last of the new period. Step A9, then, determines whether the system control unit should feed fuel to the mixing tank. If the third exceeds the fourth that means trend down, then the algorithm goes back to step A2, and system control unit signals fuel feeding unit to inject fuel to the mixing tank. If the third is smaller than the fourth characteristic value, then the algorithm returns to step A7 to explore the most recent period, to determine an updated third characteristic value. Then step A8 is repeated to determine an updated fourth characteristic value at the end of the most recent period. Again, step A9 compares the third with the fourth characteristic values. If the third exceeds the fourth, then the algorithm returns to step A2 to feed fuel to the mixing tank and the whole flow start again. Through the continuous comparison process, the repeated flow steps A7–A9 aid in consuming and regulating the excess fuel accumulated in the early cycles.

The scheme with the change of the methanol concentration and the corresponding cell characteristics value after each injection of pure methanol is briefly described below.

When the system control unit signals to inject an amount of methanol to the mixing tank, the operating characteristics begin to go upward normally due to the increasing of methanol concentration. Meanwhile, owing to the methanol crossover, the mixed potential occurring at cathode builds up gradually and lowers the operating characteristics. As shown in Fig. 7(a), every

peak (except the two peaks caused by the injection delay) is the superposition of the aforementioned two trends and caused by the discrete time injections of neat methanol. If the concentration is just enough, then the downward trend will approximately like a linear decay. If there is excess fuel accumulated, then the operating characteristics will go downward like most of the peaks shown in Fig. 7(a). With time passing away, the fuel is consumed gradually, and the mixed potential effect is reduced. Therefore, the operating characteristics will go downward, experience the minimum values and then go upward. If the trend is going upward at the end of the specific monitoring period, it means that there is excess fuel accumulated, and the system control unit stop injecting neat methanol until the excess fuel is consumed and the trend is going downward. On the contrary, if the trend is going downward at the end of the specific monitoring period, that means the fuel concentration is insufficient, then the system control unit injects the neat methanol at the same time.

2.4. Test apparatus for evaluation of the IR-DTFI control algorithm

Fig. 4 shows the system diagram of the IR-DTFI control algorithm for the operation of a direct methanol fuel cell, the system comprising:

(1) An electronic load system (Chroma, 63030) was used to measure polarization curve and served as a steady load to evaluate the performance of the IR-DTFI control algorithm.
(2) A feed pump in fluid transmission with a pure methanol reservoir and a mixing tank was applied to inject pure methanol to mixing tank.
(3) A circulation pump in fluid transmission with the mixing tank and a direct methanol fuel cell assembly was used to deliver the methanol solution and the flow rate was obtained by weighing the fuel delivered per minute.
(4) A pulse generator (GW INSTEK PHS-3610) was actuated by a microprocessor or a computer to generate pulse to drive the pumps described above.
(5) A small mixing tank was applied to mix the neat methanol with pure water to a predetermined concentration range, wherein the bubble produced from anode outlet could be used to create turbulence thereby increase the mixing rate and consume no extra power.
(6) A measurement system setup for the analysis was controlled through a personal computer with homemade software written in LabVIEW. Two programmable power supply were controlled to drive the feed pump and water pump. An electronic load and a DVD player were applied alternatively as the steady load. National Instrument USB9221, USB9215 and Tektronix AC/DC current probe A622 were used for measuring voltage and current. NI USB9211 and two *k*-type thermocouples were applied for temperature measurement. Neat methanol was used herein as a fuel and air as an oxidant. A digital refractometer #PA203, manufactured by Misco Cooperation, was adopted externally to measure the concentration of the methanol solution sampled from the inlet of anode compartment. A discrete time-pulsed fuel injection method was developed to enable the DMFC power pack system to inject pure methanol into the mixing tank for a short duration when the operating characteristic was below a calculated value. The duration of the injection was proportional to the quantity of pure methanol that was injected to the mixing tank. The controlling algorithm can be implemented using a microprocessor, such as the 8051 microprocessor for portable devices and is simple and cost-effective. The measurements verify the performance of the IR-DTFI control strategy. All experiments were conducted at room temperature (21–28 °C) at a relative humidity of 50–80% under the normal ambient conditions of portable electronic devices. As shown in Fig. 4, the stack temperature is affected by the condenser and the stack itself so that the stack will operate in a self-heating mode. The system

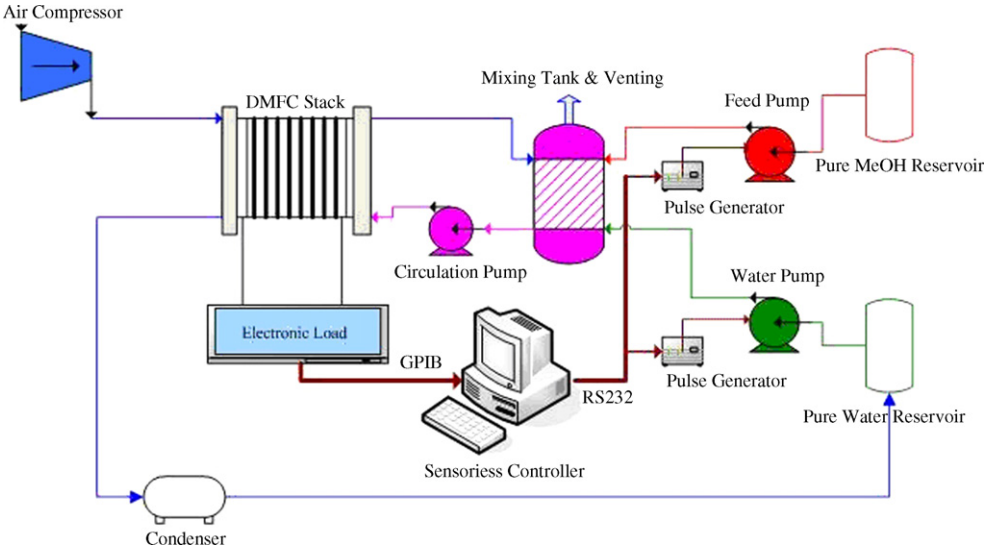

Fig. 4. Test apparatus for evaluation of the IR-DTFI control algorithm.

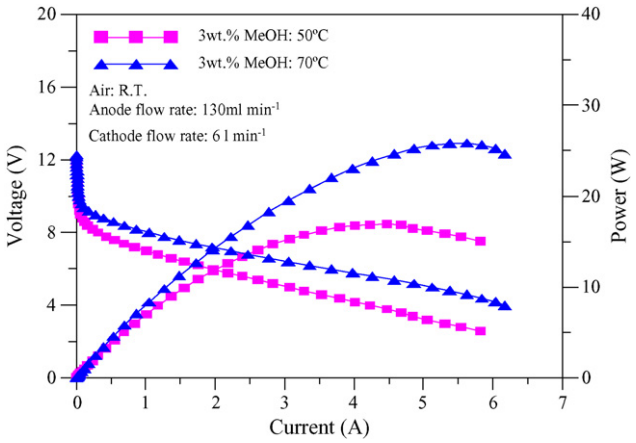

Fig. 5. Polarization curve of the stack (temperature 50 °C, 70 °C; anode flow rate, 130 ml min^{-1}; cathode flow rate, 6 l min^{-1}).

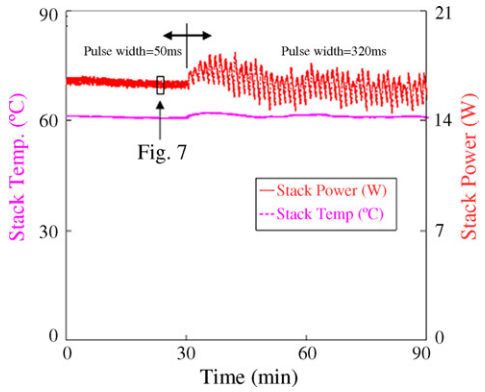

Fig. 6. Power curve variation due to methanol injection delay by the IR-DTFI control algorithm (temperature 25–65 °C; anode flow rate, 130 ml min^{-1}; cathode flow rate, 6 l min^{-1}; electronic load, constant voltage, 8 V).

control unit controls the supply of water at a fix rate, about 0.1 cm^3 min^{-1} that was determined experimentally. The fuel feeding referred to in this study is mainly the feeding of neat methanol.

3. Results and discussion

3.1. Open circuit voltage test and polarization test of the stack

The stack of 16 cells (No. 1) generated an open circuit voltage (OCV) with a mean cell voltage of 0.68 V. The OCV value can be employed to judge the initial status of the DMFC system at start-up. If the OCV is below a certain threshold, then the fuel cell power generating system will experience some trouble. The OCV can be regarded as an index to verify the functioning of the DMFC system. Fig. 5 plots the polarization curves of the stack tested on an electronic load at 50 °C and 70 °C; the methanol concentration is maintained at 3 wt.% throughout the test. The cell temperature was controlled through the methanol solution that is regulated by a temperature controller and a heater. The temperature of the fuel solution was measured at the inlet of the anode compartment. The stack typically generated a 17 W mean power output at 50 °C.

3.2. Verification of the IR-DTFI control algorithm

Various factors govern the performance of a DMFC system, such as methanol concentration, operating temperature, the manufacturing of the stacks and the loading conditions. Experiments were designed systematically based on the above factors to verify the effectiveness of the IR-DTFI control algorithm. The refractometer was used to measure the methanol concentration externally to verify the control algorithm. That assisted in getting insight of the variation of methanol concentration during the tests. The details are as follows.

3.2.1. Effect of methanol injection quantity and delay time between two injections

The methanol concentration is one of the most important factors that influence the performance of DMFCs. The methanol concentration in the experiment was controlled by varying the quantity injected and the duration between two injections. The injection quantity is determined by the pulse width that drives the fuel pump. Fig. 6 plots the power and temperature curves of a stack of 25 cells (No. 2) for two injection quantities. The pulse widths were set by controlling the programmable DC power supply using a system controller. The discharging condition was set at constant current 2 A in the electronic load. The control algorithm leads to power fluctuations that are the key feature of the IR-DTFI control scheme. These fluctuations were measured at the stack terminal and could be regulated through the conditioning circuit for the load or could be lessened by reducing the pulse width that drives the feeding pump. As shown in Fig. 6, with pulse widths set to 50 ms and 320 ms, respectively, the ratios of the amplitude of the power oscillation to the mean power were 1.9% and 20%. The wider the pulse width, the larger the power oscillation. The temperature variations associated with these two curves are 0.5 °C and 1.2 °C, respectively.

Fig. 7(a and b) represents portions of Fig. 6 with expanded x scales. The time delay between the two injections of neat methanol into the mixing tank was about 70 s. The pumping duration and delay time were adjusted to meet the requirements of a specific load. As presented in Fig. 7(a), both methanol injection delays show because excess methanol accumulated in the early cycles of the normal injection and finally the amount of excess fuel was regulated during the injection delay cycle. Every peak in the power curve was an instant response to the injection of neat methanol. As shown in Fig. 7(b), the system injected fuel at point T_0, T_1 and T_3. The concentration measured after the injection of fuel like point T_1 is about 1.2 wt.% and before the injection of fuel like point T_3, 0.7 wt.%.

3.2.2. Effect of operating temperature

Fig. 8 plots the stack power curves at two temperatures. The stack's temperatures were controlled at two levels by a fan and self-heat. The discharge condition is set at constant voltage (8 V) by the electronic load. The ratio of the amplitudes of the power oscillation to the mean power were 4% and 5% according to the 50 °C and 60 °C curves. The power fluctuations in Figs. 6 and 8 reveal two important facts. The first is that the fuel injection

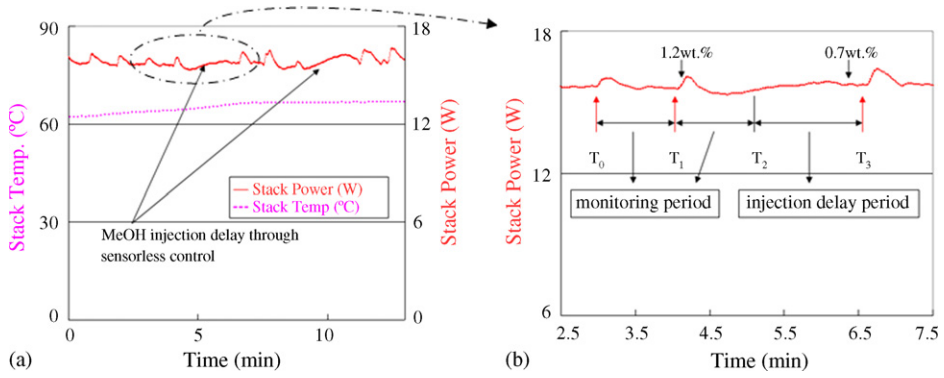

Fig. 7. Portions of Fig. 6 shows the regulation of methanol concentration by the IR-DTFI control algorithm.

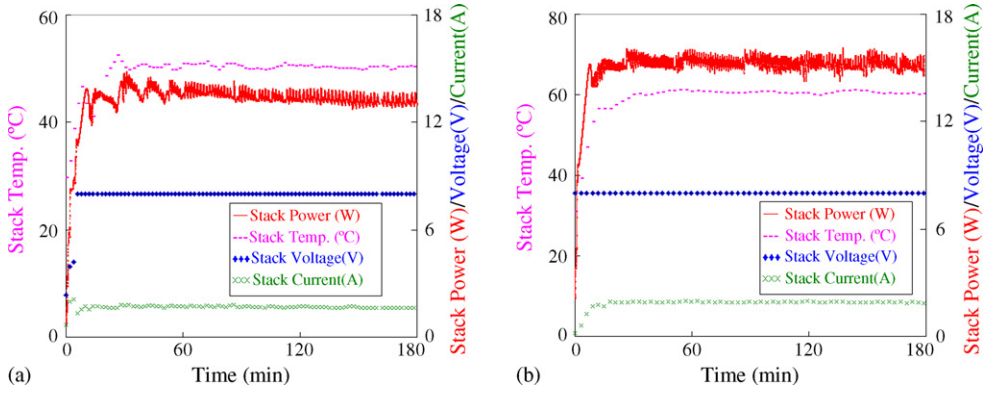

Fig. 8. Performance variation by two temperatures (a) 50 °C and (b) 60 °C, electronic load, constant voltage mode, 8 V.

quantity set by the pulse width and the pulse delay can dominate the stack power oscillation. The second is that the temperature of the stack or the environment does not influence the control stability or accuracy of the IR-DTFI control algorithm significantly.

3.2.3. *Effect of loading by electronic load*

One of the most common applications of the DMFC power source is as a charger. A charger generally utilizes three modes—constant current mode, constant voltage mode and pulse mode. The charger is normally designed to switch automatically among these three charging modes, according to the charge strategy. When DMFCs are applied as power sources for electronic products such as DVD players, PDAs or laptops, the loads act roughly like constant resistances. Accordingly, the electronic load is set in the modes (except pulse mode) mentioned above in order to confirm that the DMFC system is under steady loads. The stack (No. 1) was a 16-cell with home-made MEAs. During the tests described in this section, methanol solution was fed at a flow rate of 130 ml min^{-1}, while air was supplied through an air pump at atmospheric pressure at a flow rate of 6 l min^{-1}.

3.2.3.1. Effect of constant voltage loading. When the electronic load is set in constant voltage mode, the load sinks the current to maintain the voltage at the programmed value. Fig. 8(b) plots the performance of the 16-cell stack in constant voltage mode at 8 V at 60 °C. The average output power of the stack in this test is 16 W. The ratio of the amplitude of the power oscillation to the average power was 5% and the temperature variation was 1.6 °C. The methanol concentration was between 0.7 wt.% and 1.2 wt.%.

3.2.3.2. Effect of constant current loading. When the electronic load is set in constant current mode, the load will sink a current according to the programmed value regardless of input voltage. Fig. 9 plots the performance of 16-cell stack under constant current mode at 0.8 A. The ratio of the amplitude of the power oscillation to the average power was 4% and the temperature variation was 1 °C. The methanol concentration was between 0.6 wt.% and 1.3 wt.%.

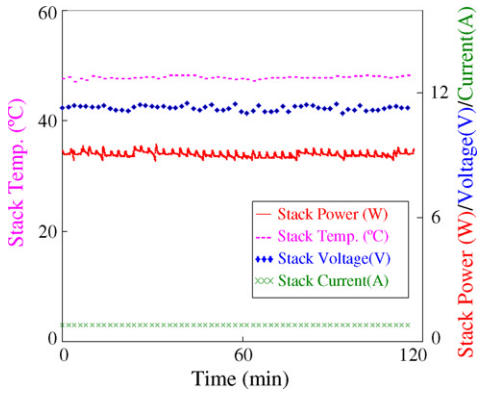

Fig. 9. Effect of constant current loading (0.8 A) set at electronic load.

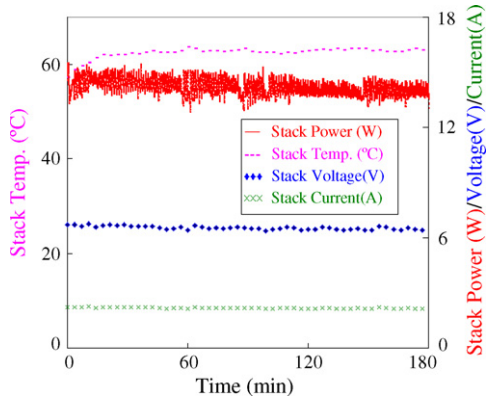

Fig. 10. Effect of constant resistance mode (3 Ω) set at electronic load.

3.2.3.3. Effect of constant resistance loading. When the electronic load is in constant resistance mode, the load will sink a current linearly proportional to input voltage according to the set-up resistance. There is a double pole RC low pass filter of input voltage, and consequently, the high frequency parts will be filtered out. Fig. 10 shows the result of loading by constant resistance mode. The resistance was programmed set at 3 Ω. The ratio of the amplitude of the power oscillation to the average power was 10% and the temperature variation was 1.8 °C. The methanol concentration was between 0.5 wt.% and 1.2 wt.%.

3.2.3.4. Short-term test. Fig. 11 plots the results for a 180 min of operation of the system. The balance temperature was within the range of 60–65 °C. The system was cold-started and reached 18 W. The pulse width used to drive the feed pump was approximately 300 ms, and the amount of methanol injected to the mixing tank was around 0.7 g. The ratio of the amplitude of the power oscillation to the mean power was under 4% that was related to the amount of methanol injected. As shown in the Fig. 11, the system was degraded at a rate of approximately 0.0143 W min^{-1}. It revealed that the IR-DTFI control algorithm could survive even if the stack had a continuous degradation.

3.2.4. Demonstration for DVD player powered by DMFC

The results shown in the above paragraphs systematically verify that the IR-DTFI control algorithm can control DMFC to act

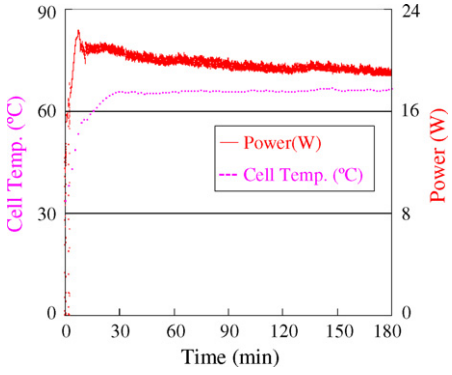

Fig. 11. 180 min test result (temperature 25–65 °C; anode flow rate, 130 ml min^{-1}; cathode flow rate, 61 min^{-1}; electronic load, constant voltage, 8 V).

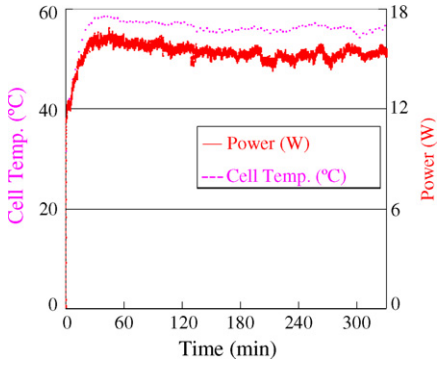

Fig. 12. DVD player test result (temperature 25–57 °C; anode flow rate, 130 ml min^{-1}; cathode flow rate, 61 min^{-1}).

like a charger in three modes set in electronic load. Additionally, a DVD player is taken as a real load for the verification of the IR-DTFI control algorithm. Fig. 12 plots the results of using a DVD player as the system load for 330 min. The BOP consumed approximately 7–8 W and the DVD player consumed 8–9 W. When the stack temperature reached 60 °C, the stack output was maintained at a stable 16 W under IR-DTFI control algorithm. The methanol concentration in the fuel was 0.7–1.2 wt.% throughout the experiment. The fuel efficiency was around 0.9–1.0 Wh cm^{-3}. The experimental results for the DVD player demonstrated that the control strategy effectively controlled the methanol concentration and was suitable for liquid feed fuel cells. From Fig. 12, the DVD player can work under power fluctuations. It is clear that these power fluctuations are manageable.

From all the experiments shown above, the methanol concentration was controlled within the range of 0.5–1.3 wt.% that was the gross result of different experiments and partly came from the measurement uncertainty of the refractometer. Despite the concentration varied about 0.8 wt.%, the methanol concentration in the range of 0.5–1.3 wt.% would not cause significant variation in the mass transport of methanol for the electrochemical reaction and the power level.

4. Conclusions

A new and original fuel sensor-less control algorithm for a liquid feed fuel cell system was presented and verified experimentally. The analysis, features, design considerations for supplying fuel of a liquid feed fuel cell system were demonstrated. The salient findings of this work are summarized as follows.

The IR-DTFI control algorithm governs the system using the operating characteristics of the liquid feed fuel cell system. Accordingly, it does not suffer from the degradation of MEAs. Experimental results for the 17 W prototypes are presented to verify the operating and control principles. Throughout a series of tests, the ratio of the power oscillation to the mean power was under 10% and the methanol concentration was controlled within the range 0.5–1.3 wt.%. A microprocessor such as the 8051 can implement the controlling algorithm in portable devices and is simple and cost-effective. Consequently,

the advantages of the IR-DTFI control algorithm, including reducing the weight and volume and the cost; extending the lifetime; increasing the reliability and simplifying the control algorithm, make the liquid feed fuel cell system highly promising for portable applications.

Acknowledgement

The authors give great thanks to the financial support from the Institute of Nuclear Energy Research (INER), Taiwan, ROC.

References

[1] H. Zhao, J. Shen, J. Zhang, H. Wang, D.P. Wilkinson, C.E. Gu, J. Power Sources 159 (2006) 626–636.
[2] S.R. Narayanan, W. Chun, T.I. Valdez, US patent 6,306,285 (2001).
[3] W.P. Acker, M.S. Adler, S. Gottesfeld, US patent 6,991,865 (2006).
[4] J. Zhang, K.M. Colbow, A. Wong, B. Lin, US patent 6,698,278 (2004).
[5] Y.J. Chiu, H.C. Lien, J. Power Sources 159 (2006) 1162–1168.
[6] C.Y. Chen, P. Yang, Y.S. Lee, K.F. Lin, J. Power Sources 141 (2005) 24–29.
[7] C.Y. Chen, P. Yang, J. Power Sources 123 (2003) 37–42.
[8] C.Y. Chen, C.S. Tsao, Int. J. Hydrogen Energy 31 (2006) 391–398.